

## Transition-Metal Coordination in Polymer Blends and Model Systems

Laurence A. Belfiore,\* Alfredo T. N. Pires,† Yinghua Wang, Hugh Graham, and Eiji Ueda‡

Department of Chemical Engineering, Polymer Physics and Engineering Laboratory, Colorado State University, Fort Collins, Colorado 80523

Received June 3, 1991; Revised Manuscript Received September 5, 1991

**ABSTRACT:** Several metal-containing polymer blends which form coordination complexes have been investigated in the solid state. The d-block model compounds are zinc salts of acetic acid, lauric acid, and stearic acid. The ligand is poly(vinylpyridine) with nitrogen in either the 2- or 4-position. Thermal analysis via differential scanning calorimetry (DSC) is used to probe the phase behavior of these binary mixtures at the macroscopic level. DSC thermograms identify the melting transition of the small-molecule-rich phase and the glass transition of the amorphous polymer-rich phase. High-resolution carbon-13 solid-state NMR spectroscopy is used in an indirect detection mode to probe microenvironmental factors that influence mixing. The interaction-sensitive carboxyl carbon resonance of the zinc salts is perturbed in blends with poly(vinylpyridine) when the nitrogen ligand is structurally accessible. The NMR data suggest that all of the small molecules form coordination complexes with poly(4-vinylpyridine) except magnesium acetate. The divalent magnesium cation is classified as a hard acid, and it favors the acetate anion and the waters of hydration, which are hard bases, instead of the pyridine ligand, which is a borderline base. d-Metal complexation is observed in polymer-ionomer blends representing a direct extension of the above-mentioned studies on model systems, particularly those for zinc stearate with either poly(2-vinylpyridine) or poly(4-vinylpyridine). As expected, carbon-13 NMR spectroscopic detection of solid-state coordination in polymer-ionomer blends yields positive results when the ionic copolymer is neutralized with zinc and when the nitrogen ligand is in the 4-position of the pyridine ring. These phenomenological observations suggest that zinc coordinates to the pyridine ring via nitrogen's lone pair and infrared spectroscopic data support the concept that the pyridine group participates in metal-ligand  $\pi$ -bonding. The stress-strain properties of poly(4-vinylpyridine)/zinc ionomer blends exhibit a synergistic mechanical performance when the nitrogen/zinc molar ratio is optimized.

### Introduction

The use of d-block metals to produce coordination complexes in polymer-polymer and polymer-small molecule blends, illustrated herein, represents an extension of the hydrogen-bonding concept that has dominated literature examples of strongly interacting systems. There are relatively few documented studies that have focused on the coordination mechanism to enhance compatibility in polymer blends. Wissbrun and Hannon<sup>1</sup> studied d-metal complexation in polymer-nitrate salt mixtures where the polymers were chosen from the following list: cellulose acetate, poly(vinyl acetate), poly(vinyl alcohol), poly(methyl acrylate), or poly(methyl methacrylate). The nitrate salts contained either copper, zinc, or cadmium cations. Agnew<sup>2</sup> prepared d-metal chloride complexes with vinylpyridines and poly(vinylpyridine). Coordination in the monomeric complexes with cobalt and zinc revealed similar geometries and coordination numbers relative to the solid polymeric complexes, but the trends were not consistent for the monomeric and polymeric complexes based on nickel and copper(II).<sup>2</sup> All of the d-metal chloride complexes with 2-vinylpyridine adopted tetrahedral arrangements. Molecular models suggest that *intramolecular* coordination between adjacent vinylpyridine monomer units is feasible in poly(2-vinylpyridine), but mostly *intermolecular* coordination should occur in poly(4-vinylpyridine).<sup>2</sup> Register et al.<sup>3</sup> investigated polymer-ionomer blends containing poly(styrene-co-4-vinylpyridine) with copper-neutralized carboxy-terminated polybutadiene and reported that substantial, though not complete, mixing occurs in the polybutadiene-rich phase.

The work described herein follows the inspirational study of Peiffer, Duvdevani, Agarwal, and Lundberg<sup>4</sup> which reports that the zinc salt of a sulfonated ethylenepropylene diene thermoplastic elastomer produces coordination complexes with random glassy copolymers of styrene and 4-vinylpyridine.<sup>4,5</sup>

The blends chosen for investigation progress smoothly from polymer-small molecule mixtures, in which the molecular weight of the alkyl tail in the zinc salts is systematically increased, to polymer-ionomer blends. The overall objective is to identify molecular engineering design concepts based on structural variations in the "model systems" and employ these concepts in the design of high-molecular-weight blends that potentially exhibit synergistic macroscopic properties. Carbon-13 solid-state NMR spectroscopy is employed in an *indirect* detection mode to probe coordination from a molecular engineering viewpoint. The carboxylate carbon NMR signal is extremely sensitive to blending-induced metal-ligand bonds formed between the zinc cation and the pyridine group. Infrared spectroscopy directly identifies the pyridine ring as a complementary interaction site, and the shift of the aromatic carbon-nitrogen stretching vibration to higher energy supports the hypothesis that the pyridine group coordinates to the metal center via  $\sigma$ -bonding and  $\pi$ -bonding. Whenever possible, the spectroscopic results are correlated with macroscopic temperature-composition phase diagrams, generated with the aid of differential scanning calorimetry.

Obtaining direct evidence for polymeric metal-ligand complexes is not a simple task, especially when coordination between a small-molecule zinc salt and an amorphous polymer is restricted to the noncrystalline regions of the blend, rendering X-ray diffraction techniques completely ineffective. The previous paragraph briefly

\* Author to whom all correspondence should be addressed.

† Federal University of Santa Catarina, Florianopolis, Brazil.

‡ Asahi Chemical Industry, Okayama, Japan.

mentions the indirect nature of carbon-13 solid-state NMR diagnostics and the direct probe offered by infrared spectroscopy. Even though NMR identifies coordination between the zinc cation and the pyridine nitrogen lone pair via the carbon nuclear spin manifold which is a few bonds removed from the interaction sites, the results correlate quite well with macroscopic phase behavior.<sup>6</sup> Infrared spectroscopy directly identifies the pyridine ring in poly(4-vinylpyridine) as a  $\pi$ -bonding ligand because the carbon–nitrogen stretching vibration, which is unique to the polymer, shifts to higher energy as a consequence of coordination.<sup>6</sup> It is envisioned that the metal d-electrons in the  $t_{2g}$  molecular orbitals overlap with the “bonding” p-orbitals of the ligand to strengthen the carbon–nitrogen bond in the pyridine ring. However, a correlation between the infrared data and macroscopic phase behavior is not attempted in this contribution because the infrared absorptions overlap extensively in the frequency region of interest. It should be mentioned that both spectroscopic techniques fail to identify a geometry, or a coordination number, for the metal–ligand complex in the blended states. X-ray crystallography identifies the zinc cation in a slightly distorted pseudooctahedral arrangement in undiluted zinc acetate dihydrate,<sup>33</sup> but a tetrahedral complex is the preferred geometry for the anhydrous crystal.<sup>7</sup> Hard-and-soft acid–base concepts<sup>8</sup> might account for the displacement of the “hard-base” water(s) of hydration in zinc acetate dihydrate by the “borderline-base” pyridine ligand, because the zinc cation is characterized as a borderline acid. Brønsted acid ionization constants<sup>9</sup> (i.e.,  $pK_a$  values) and Guttmann donor–acceptor numbers<sup>10</sup> rank the pyridine ligand as a stronger base than the waters of hydration. Hence, stronger metal–ligand  $\sigma$ -bonding is expected in zinc acetate–poly(4-vinylpyridine) complexes relative to zinc acetate dihydrate, and this trend favors an increase in the pseudooctahedral ligand field splitting.<sup>11</sup> However, this claim cannot be verified by d–d electronic transitions that absorb radiation in the visible and/or near-infrared region of the spectrum because  $Zn^{2+}$  forms a  $d^{10}$  complex with a completely filled d-subshell.<sup>12</sup> Since complexation is restricted to the amorphous regions of the polymer–small molecule blends, long-range periodicity is not required, and, hence, the nature of the complex may not be well-defined. In support of this claim, solid-state NMR consistently identifies a rather broad, but well-resolved, signal for the carboxylate carbon of the zinc salts and the zinc-neutralized copolymer in the vicinity of 179–181 ppm when binaries are produced that contain poly(vinylpyridine) with a structurally accessible nitrogen-like molecular orbital containing the lone pair.<sup>6,13,14</sup>

## Experimental Procedures

**Materials.** Poly(2-vinylpyridine) (P2VP) and poly(4-vinylpyridine) (P4VP) were purchased from Scientific Polymer Products with reported viscosity-average molecular weights of  $5 \times 10^4$  and  $4 \times 10^4$ , respectively. These relatively low-molecular-weight polymers were blended with small-molecule zinc and magnesium salts. Zinc acetate dihydrate,  $Zn(OOCH_3)_2(H_2O)_2$ , was acquired from Sigma Chemical Co., anhydrous zinc laurate,  $Zn(OOCC_{11}H_{23})_2$ , was purchased from Pfaltz & Bauer, anhydrous zinc stearate,  $Zn(OOCC_{18}H_{37})_2$ , was supplied by Alfa Products, and magnesium acetate tetrahydrate,  $Mg(OOCH_3)_2(H_2O)_4$ , was obtained from Aldrich Chemical Co. Zinc-neutralized copolymers of ethylene and methacrylic acid (15 wt % acid, 60% neutralization of the carboxylate groups, tradename Surlyn 1706) were kindly provided by Ruskin Longworth and George Hoh at E. I. Du Pont de Nemours and Co. in Wilmington, DE. All materials were used without further purification or neutralization in the case of the ionic copolymers. The solvents used for blend preparation were reagent grade.

**Table I**  
Metal-Containing Model Binary Systems Investigated

metal salts	polymer	solvent	molding temp, °C
zinc acetate	P4VP	acetic acid, 2%	250
zinc laurate	P4VP	THF–CH <sub>2</sub> Cl <sub>2</sub>	none
zinc stearate	P4VP	methylene chloride	150
zinc stearate	P2VP	methylene chloride	150
magnesium acetate	P4VP	methanol	130

**Sample Preparation Techniques.** Polymer–small molecule blends were mixed initially in solution for at least 24 h without the formation of a precipitate followed by solvent evaporation in a fume hood. The residues were compression-molded a minimum of three times in a Carver laboratory press at the temperatures indicated in Table I with subsequent slow-cooling to ambient temperature until macroscopic uniformity was obtained. All blends were dried further under vacuum at 25 °C for at least 1 week before physical characterization was attempted. Solvents and compression-molding temperatures for each polymer–small-molecule “model” system are summarized in Table I. Polymer-ionomer blends of Du Pont’s Surlyn zinc-containing ethylene–methacrylic acid copolymer with either P2VP or P4VP were prepared from direct molten mixing in a Carver laboratory press at 200 °C.

## Physical Characterization Methods

**Differential Scanning Calorimetry.** Thermal analysis was performed on a Perkin-Elmer DSC-7 with the overall goal of generating temperature–composition phase diagrams. Melting endotherms were recorded under helium and nitrogen purges at a rate of 10 °C/min during the first heating trace in the calorimeter. After quenching from the molten state, glass transition temperatures were measured at a rate of 20 °C/min during the second heating trace.  $T_g$  was calculated at the midpoint of the heat capacity change between the liquid and glassy states, without complicating effects due to enthalpy relaxation. Differential power output was monitored via Perkin-Elmer’s TAC-7/DX thermal analysis controller in conjunction with the DSC-7 multitasking software on a 386/33 personal computer.

**Carbon-13 Solid-State NMR Spectroscopy.** Proton-enhanced dipolar-decoupled carbon-13 solid-state NMR spectra were obtained on a modified Nicolet NT-150 spectrometer at the NSF-supported Regional NMR Center, Colorado State University, Fort Collins, CO. The carbon frequency was 37.735 MHz, and magic-angle spinning was performed at 3600 Hz. The spectrometer incorporates a cross-polarization/magic-angle-spinning (CP/MAS) probe that was designed and constructed at the CSU Regional NMR Center. The spinner system is a modified version of Wind’s<sup>15</sup> with a sample volume of 0.3 cm<sup>3</sup>. A proton 90° pulse width of 5  $\mu$ s was employed, corresponding to a radio-frequency (rf) field strength of 50 kHz. The rf field was maintained at 50 kHz during cross polarization and subsequent high-power <sup>1</sup>H decoupling. The <sup>1</sup>H–<sup>13</sup>C cross-polarization contact time was typically 1–2 ms, and the pulse sequence repetition delay was 2 s. In consideration of the fact that proton spin-lattice relaxation times in the laboratory frame are much less than 1 s for the materials of interest, the <sup>13</sup>C NMR spectra are fully relaxed and contain information about all regions of the sample that respond to a contact time of 1–2 ms. The <sup>13</sup>C free induction decay (FID) was accumulated via 2K time-domain data points using quadrature detection. Prior to Fourier transformation, the signal-averaged FID was zero-filled to 4K. The spectral width encompassed a  $\pm 10$ -kHz frequency range, and 5 Hz of line broadening was employed. Following Stejskal and

Schaefer,<sup>16</sup> spin-temperature alternation in the rotating frame was used to suppress the buildup of artifacts which may occur in proton-enhanced spectra. The sample temperature was maintained at  $15 \pm 2$  °C by passing the spinner air through a copper cooling coil immersed in an ice bath. Carbon-13 chemical shifts were referenced externally to the methyl resonance of hexamethylbenzene, 17.355 ppm deshielded from tetramethylsilane (TMS).<sup>17</sup>

**Fourier Transform Infrared Spectroscopy.** Thin films for FTIR measurements were cast from solution onto zinc sulfide windows at ambient temperature. After the majority of the solvent evaporated, the films were transferred to a vacuum oven at 60–70 °C for more than 72 h to remove residual solvent, with subsequent storage under vacuum. Infrared spectra were recorded on a Perkin-Elmer Model 1600 FTIR spectrophotometer. A minimum of 64 scans was signal averaged at a resolution of 4  $\text{cm}^{-1}$ . The experiments were carried out at room temperature ( $\approx 20$  °C). All of the films used for infrared studies were sufficiently thin to be within the range where the Beer-Lambert law<sup>18</sup> is obeyed.

**Mechanical Properties.** Ambient-temperature stress-strain properties were measured on a servohydraulic Instron Model 8501 tensile testing apparatus at a draw rate of  $8 \times 10^{-3}$  in./s. Waveform generation and digital data acquisition were accomplished via the FLAPS (Fatigue Laboratory Applications) software package and an IEEE-488 instrumentation interface on a Compaq Deskpro 386/20 personal computer. The sample thickness was  $\approx (7-8) \times 10^{-3}$  in., and the initial length of the ASTM (D 638M) specimen was 0.4 in. Tensile stress in these samples was detected on a 20-lb low-force load cell.

## Results and Discussion

**Transition-Metal Coordination in Polymer-Small Molecule Blends. Zinc Acetate and Poly(4-vinylpyridine).** Carbon-13 NMR spectroscopy is employed herein as a diagnostic probe of d-metal complexes in the solid state. The nitrogen lone pair in P4VP is available to form a coordination complex with the d-orbitals of the zinc cation.<sup>10-12</sup> Accessibility to the nitrogen ligand in the 2- vs 4-position of the pyridine ring is an important consideration in the chemical design of these strongly interacting systems. Zinc acetate was chosen as the transition-metal component because (i) due to its reasonably low melting temperature ( $\approx 245$  °C) in comparison with other zinc salts, homogeneous films can be produced from binary mixtures via high-temperature compression molding without inducing thermal degradation of poly(vinylpyridine) and (ii) the conformation of the organic portion of the molecule ( $\text{OOCCH}_3$ )<sub>2</sub> is not expected to hinder potential coordination with the pyridine ligand. In the following sections, the molecular weight of the alkyl tail in the zinc salt is increased from C<sub>1</sub> to C<sub>11</sub> to C<sub>18</sub>, and NMR spectra of the carboxylate carbon depend on this structural change in blends with poly(vinylpyridines).

Zinc acetate and poly(4-vinylpyridine) precipitate from methanol<sup>19</sup> but not from acetic acid. The solid-state data described below were obtained from acetic acid-cast films followed by subsequent high-temperature compression molding as indicated in the Experimental Section. The concentration dependence of the glass transition temperature is illustrated in Figure 1 for these binary mixtures. Synergistic thermal response is observed in the vicinity of 10–30 mol % zinc acetate where  $T_g$  of the blends is greater than that of undiluted poly(4-vinylpyridine). The maximum enhancement in  $T_g$  is approximately 20 °C when

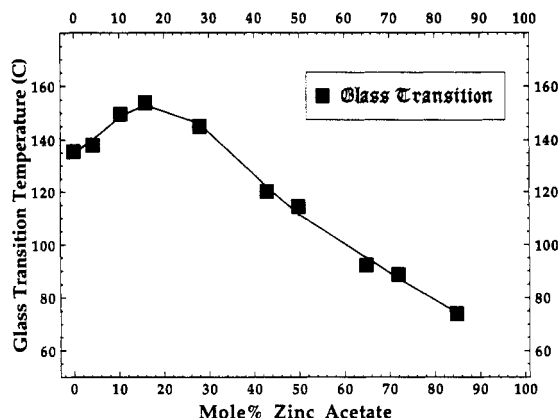


**Figure 1.** Synergistic thermal response in the glass transition phase diagram for binary mixtures of zinc acetate and poly(4-vinylpyridine). The enhancement of  $T_g$  is  $\approx 20$  °C relative to undiluted P4VP. No evidence of melting is observed for blends that contain as much as 85 mol % zinc acetate.

the molar concentration of zinc acetate is  $\approx 16$ %. Furthermore, the first-order melting transition of the potentially crystallizable zinc salt is not observed for blends containing as much as 85 mol % zinc acetate. These results suggest that (i) the two components form macroscopically compatible amorphous mixtures and (ii) d-metal coordination is operative based on the fact that the zinc salt increases the glass transition temperature of the blends when the polymer is in excess. Frechet et al.<sup>20</sup> measured synergistic glass transition response in polymer-polymer blends of poly(4-vinylpyridine) with poly(vinylphenol), presumably due to the formation of hydrogen bonds. Kwei and co-workers<sup>21-25</sup> have identified several interpolymer complexes that exhibit synergistic behavior in the glass transition phase diagram. To illustrate the importance of structural variations in the pyridine ring, blends of zinc acetate with poly(2-vinylpyridine) exhibit a melting transition when the concentration of the zinc salt ranges from 40 to 100 mol %.<sup>26</sup> Furthermore, the glass transition of P2VP is very weakly concentration dependent in mixtures with zinc acetate.<sup>26</sup> These observations from thermal analysis indicate that two-phase behavior is prevalent when the nitrogen lone pair is sterically hindered to some extent, as it is in the case of poly(2-vinylpyridine). However, infrared spectroscopy detects evidence for metal-ligand bonding in the miscible fraction of zinc acetate and poly-(2-vinylpyridine).<sup>27</sup>

Molecular-level support for the synergistic glass transition response in blends of zinc acetate with P4VP is provided in Figure 2. High-resolution solid-state NMR spectra in the carboxylate carbon chemical shift region, which is unique to zinc acetate, reveal that the relatively sharp resonance in the vicinity of 185 ppm is broadened and shifted gradually to 179 ppm as zinc acetate is diluted by the polymer. There is no <sup>13</sup>C NMR evidence in Figure 2 for the coexistence of both crystalline and amorphous phases that contain spectroscopically detectable fractions of zinc acetate. Comparison of the full width at half-height for zinc acetate's carboxylate carbon signal suggests that the blends depicted in the lower eight spectra of Figure 2 are amorphous and compatible. This claim, supported by DSC, is based on the breadth of the resonance envelope for blends containing 10–85 mol % zinc acetate relative to the uppermost spectrum of the completely crystalline small molecule which was prepared from acetic acid solution and high-temperature compression molding, analogous to the blends. In the four lowermost spectra of Figure 2 at 10, 16, 28, and 34 mol % zinc acetate, a shoulder appears on the carboxylate carbon signal in the vicinity

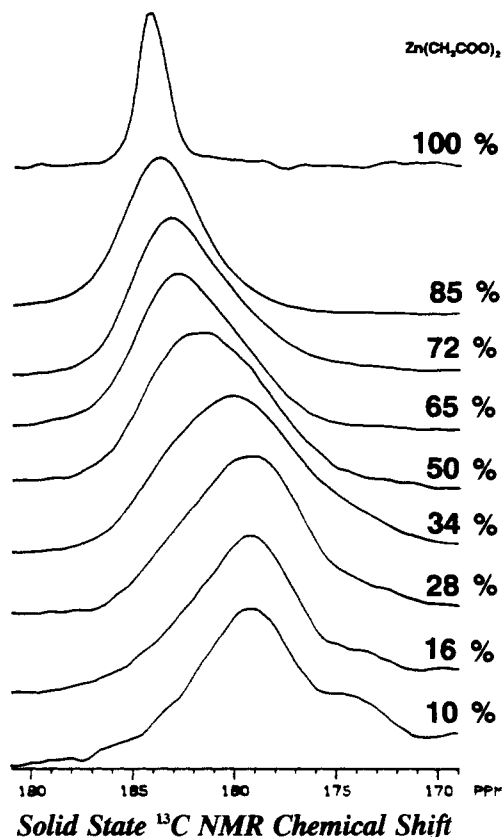


**Figure 2.** Carbon-13 solid-state NMR spectra in the carboxylate chemical shift region for binary mixtures of zinc acetate and poly(4-vinylpyridine). The mole percent of zinc acetate is indicated at the right of each spectrum. The broad resonance at  $\approx 180$  ppm in the lower spectra is indicative of zinc coordinated to the pyridine ring via the nitrogen lone pair.

of 170–175 ppm. This is attributed to zinc acetate coordinated to two pyridine ligands in a pseudooctahedral geometry when the polymer is present in excess. Both hard-and-soft acid-base considerations<sup>8</sup> and a ranking of the strength of the possible ligand bases<sup>9,10</sup> suggest that zinc acetate dihydrate will shed one or both of its waters of hydration and coordinate to pyridine in an effort to stabilize the complexes via stronger metal-ligand  $\sigma$ -bonding. If the zinc salt forms metal-ligand bonds with pyridine groups on two different macromolecular chains, then the enhancement of the glass transition temperature is rationalized via "coordination cross-links". Synergistic thermal response is observed in Figure 1 for the coordination complexes whose  $^{13}\text{C}$  NMR data are illustrated in the lower three spectra of Figure 2. The proposed phenomenological correlation between macroscopic and site-specific probes of metal-ligand complexation in these model blends is evident from the following observation. When  $T_g$  of the blends exceeds that of the undiluted polymer (i.e., for concentrations of zinc acetate between 10 and  $\approx 35$  mol %), the peak of the broad carboxylate carbon signal is found at 179 ppm and traces of the above-mentioned shoulder are present between 170 and 175 ppm. At higher concentrations of zinc acetate when the  $T_g$ -composition data in Figure 1 reveal that the glass transition of the blends no longer surpasses that of the undiluted polymer, the peak position of the carboxylate resonance is found at progressively higher chemical shifts which approach 185 ppm, characteristic of completely crystalline zinc acetate. Furthermore, the shoulder at 170–175 ppm on the carboxylate carbon resonance is absent for blends that contain more than 34 mol % zinc acetate, suggesting that the metal center coordinates to one pyridine group

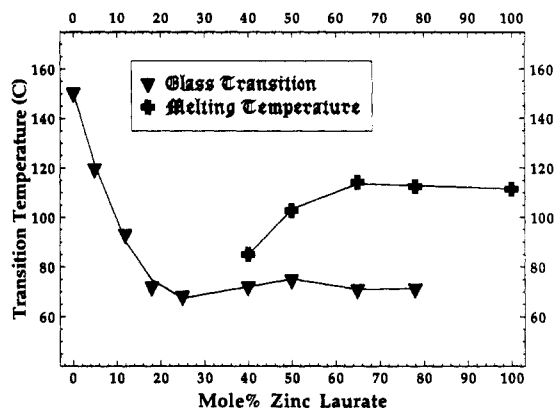


**Figure 3.** Temperature-composition phase diagram illustrating melting and glass transition response for binary mixtures of zinc laurate and poly(4-vinylpyridine). Synergistic behavior is not observed.

in this range of blend concentrations. Complementary NMR spectral perturbations (not illustrated in Figure 2) between 145 and 165 ppm are also observed for the pyridine ring carbons in P4VP when the complexes contain 25–85 mol % zinc acetate.<sup>26</sup>

**Zinc Laurate and Poly(4-vinylpyridine).** The interaction-sensitive carboxylate carbon resonance of the zinc-containing small molecule is useful to correlate site-specific results from solid-state NMR with the temperature-composition projection of the phase diagram for blends containing zinc laurate and P4VP. In a previous investigation that originated in this laboratory, the carboxylate carbon NMR signal of the liquid-crystalline component, *p*-(pentyloxy)cinnamic acid, was correlated phenomenologically with the two-phase behavior of solid-state blends containing Bisphenol A polycarbonate.<sup>28</sup> Results from  $^{13}\text{C}$  solid-state NMR spectroscopy and differential scanning calorimetry identify two-phase behavior over a wide concentration range for blends of zinc laurate with P4VP. The conformation of the rather long organic portion of zinc laurate prevents NMR-detectable coordination with the polymer when the nitrogen lone pair is in the 2-position of the pyridine ring. However, the interaction can be detected spectroscopically when the lone pair is structurally accessible in the case of poly(4-vinylpyridine). This observation suggests that nitrogen's lone pair plays a more important role in coordination phenomena than the  $\pi$ -orbitals of the pyridine ring. Due to solubility limitations, blends of zinc laurate and P4VP were cast from a cosolvent mixture of tetrahydrofuran and methylene chloride at ambient temperature, as indicated in Table I. Precipitation did not occur from the cosolvent mixtures.

The concentration dependence of  $T_g$  and  $T_m$  is illustrated in Figure 3. The melting transition of the small-molecule-rich phase was measured at a DSC heating rate of 10 °C/min during the first heating cycle in the calorimeter, and the second-order transition characteristic of the polymer-rich phase was observed at 20 °C/min during the second heating cycle after quenching from the molten state into liquid nitrogen. Both  $T_g$  and  $T_m$  are depressed with no evidence of synergism. d-Metal coordination is detectable via the carboxylate carbon resonance of zinc laurate as illustrated in the NMR spectra of Figure 4. There are two contributors to the overall resonance envelope of zinc laurate's carboxylate carbon that appear to be separated by  $\approx 4$  ppm. The relatively sharp signal in the vicinity of 185 ppm is characteristic of completely crystalline zinc laurate. Generation of a coordination complex between the

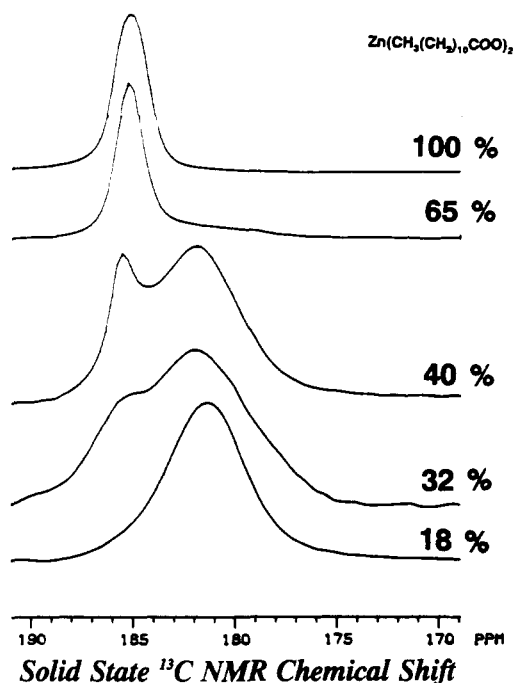


**Figure 4.** Carbon-13 solid-state NMR spectra in the carboxylate chemical shift region for binary mixtures of zinc laurate and poly(4-vinylpyridine). The mole percent of zinc laurate is indicated at the right of each spectrum. The weak carboxylate signal at 185 ppm in the 32 mol % zinc laurate spectrum is indicative of a highly disordered crystalline phase in low abundance.

two dissimilar components produces a new mixing-induced signal at  $\approx 181$  ppm when P4VP is the dominant component. The breadth of the 181 ppm resonance relative to the sharp signal at 185 ppm suggests that the interactions are concentrated in the amorphous phase. Hence, long-range crystallographic order is not required to produce coordination complexes in polymer-small molecule systems. It should be emphasized that the carboxylate resonance envelope in blends of zinc laurate with P4VP differs from the NMR data in the previous section for blends of zinc acetate with P4VP due to phase diagram dissimilarities and the fact that the carboxylate carbon signal is sensitive to the phase or phases that contain the zinc salt. Whereas blends of zinc acetate and P4VP are amorphous and compatible, with the carboxylate signal exhibiting a full width at half-height of 4–7 ppm as illustrated in Figure 2, blends of zinc laurate and P4VP exhibit concentration-dependent miscibility with two coexisting solid-state phases present over most of the concentration range at the temperature of the NMR experiment ( $\approx 15^\circ\text{C}$ ). The carboxylate resonance envelope of zinc laurate in Figure 4 is consistent with the two-phase behavior of the blends discussed in this section, and the NMR line widths are representative of crystalline (185 ppm) and metal-ligand-coordinated amorphous (181 ppm) microenvironments. Two-phase behavior is observed from the viewpoint of solid-state NMR (Figure 4) at 32, 40, and 65 mol % zinc laurate where the crystalline and rigid amorphous phases are detected simultaneously. Melting transitions are detected in the DSC thermograms for blends containing 40–100 mol % zinc laurate. The appearance of the unresolved shoulder at 185 ppm in the NMR spectrum at 32 mol % zinc laurate suggests that solid-state NMR can detect the crystalline phase, which is in low abundance and might be slightly disordered, while the DSC thermogram for this mixture is dominated by the glass transition process in the 60–70  $^\circ\text{C}$  temperature range. The liquidus line representing  $T_m$  depression

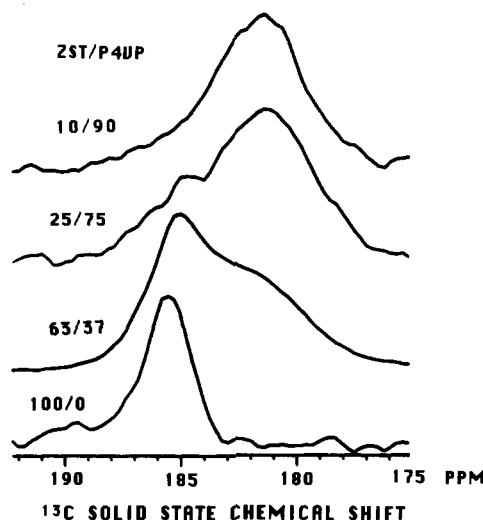


**Figure 5.** Carbon-13 solid-state NMR spectra in the carboxylate chemical shift region for binary mixtures of zinc stearate and poly(4-vinylpyridine). The mole percent of zinc stearate-P4VP is indicated at the left of each spectrum. The NMR-detectable two-phase behavior of this system is spectroscopically similar to blends of zinc laurate with P4VP.

converges on the concentration-insensitive glass transition phase boundary in the vicinity of 30–35 mol % zinc laurate (see Figure 3). This poses a mobility restriction for crystallization of the 32 mol % blend, thereby retarding the kinetics which govern crystallization of the small-molecule-rich phase from the molten state. The zinc laurate-P4VP binary system represents one of a number of investigations originating in this laboratory that have produced temperature-composition phase diagrams similar to the one illustrated in Figure 3. Four strongly interacting partially miscible semicrystalline binary systems that have been identified previously are *resorcinol* with poly(2-vinylpyridine),<sup>29</sup> *poly(ethylene oxide)* with poly(vinylphenol),<sup>30</sup> *poly(ethylene succinate)* with poly(vinylphenol),<sup>31</sup> and *poly(ethylene adipate)* with poly(vinylphenol).<sup>32</sup> In each case study, the melting-point depression line approaches the single glass transition phase boundary with increasing concentration of the amorphous component such that the restricted range of plausible supercooling temperatures coupled with the decrease in chain mobility upon cooling in the vicinity of  $T_g$  thwarts the crystallization process of the potentially crystallizable component (italicized for each of the five cases mentioned above).

In both of the polymer-zinc salt blends discussed above, the rather broad carboxylate carbon resonance in the vicinity of 180 ppm is an indicator of metal-ligand coordination in the amorphous phase between the d-orbitals of the zinc cation and the structurally accessible nitrogen lone pair.

**Zinc Stearate and Poly(vinylpyridines).** In this section, the alkyl tail of the zinc salt is extended to an 18-carbon linear chain. The effect of this structural modification on the potential for zinc stearate to form a coordination complex with poly(vinylpyridines) is detected quite convincingly from  $^{13}\text{C}$  solid-state NMR spectroscopy of the carboxylate signal. Structural accessibility of the pyridine nitrogen lone pair is an important consideration in the chemical design of strongly interacting blends that contain poly(vinylpyridine). This concept is illustrated below by focusing on the NMR line shape of zinc stearate's carboxylate carbon resonance in blends with P2VP vs P4VP.

$^{13}\text{C}$  NMR spectra are presented in Figure 5 for meth-

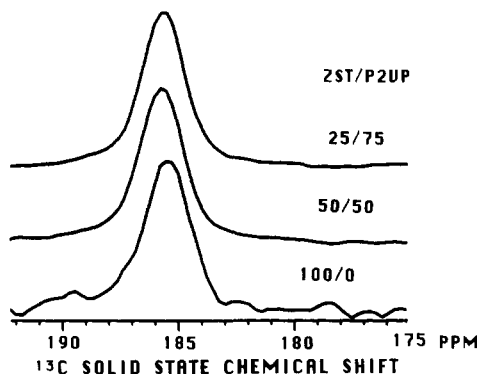


**Figure 6.** Carbon-13 solid-state NMR spectra in the carboxylate chemical shift region for binary mixtures of zinc stearate and poly(2-vinylpyridine). The mole percent of zinc stearate-P2VP is indicated at the right of each spectrum. The carboxylate signal of zinc stearate is spectroscopically inert in all of the blends.

ylene chloride-cast blends of zinc stearate and P4VP that were subsequently molded at 150 °C. The data can be categorized with the results in the previous section for two-phase mixtures of zinc laurate and P4VP. The carboxylate carbon signal of zinc stearate in Figure 5 reveals that there are at least two contributors to its resonance envelope. This suggests that two NMR-dissimilar zinc stearate-containing phases coexist when the concentration of the small molecule is between 25 and 63 mol %. On the basis of observation of zinc stearate's carboxylate signal in Figure 5, the crystalline (185–186 ppm) and metal-ligand-coordinated amorphous (181–182 ppm) phases are detected simultaneously in two of the blends. Assignments are made from a comparison of peak position and line width relative to the carboxylate signal in undiluted zinc stearate (lowermost spectrum in Figure 5). When the structure of the polymeric component is altered such that the potential nitrogen ligand is in the 2-position of the pyridine ring,  $^{13}\text{C}$  solid-state NMR spectra illustrated in Figure 6 reveal that the carboxylate signal between 185 and 186 ppm is spectroscopically inert in blends of zinc stearate and P2VP. The data suggest that structural inaccessibility of the P2VP nitrogen lone pair due to steric hindrance of the polymeric backbone coupled with the rather long aliphatic tail of zinc stearate prevents the formation of a coordination complex with the zinc cation in the amorphous phase. Results from infrared spectroscopy provide evidence for metal-ligand bonding when the nitrogen lone pair is in the 4-position (i.e., P4VP), but there is no similar evidence when the lone pair is in the 2-position (i.e., P2VP).<sup>27</sup> Consequently, zinc stearate's carboxylate carbon resonance does not exhibit a relatively broad amorphous component in the 181–182 ppm chemical shift region in blends with P2VP (see Figure 6), and it is postulated that the zinc salt forms isolated crystalline domains in the blended states.

**Fourier Transform Infrared Spectroscopic Investigation of the Coordination Complexes.** The macroscopic and molecular-level results discussed above in terms of transition-metal coordination as a potential route for preparing compatibilized blends are supported further by FTIR data of the ligand in Figure 7. Analogous to the results of Peiffer et al.,<sup>4</sup> there are two aromatic carbon-nitrogen stretching vibrations in P4VP that exhibit sensitivity to microenvironmental factors. Infrared bands are observed at 1596  $\text{cm}^{-1}$  when coordination is absent and 1617  $\text{cm}^{-1}$  when coordination is operative in blends with zinc acetate (Figure 7a) and zinc laurate (Figure 7b). The absorption band at 1617  $\text{cm}^{-1}$  is absent in all of the

undiluted starting materials. This difference of approximately 20 wavenumbers between two distinct carbon-nitrogen absorption modes suggests qualitatively that the pyridine group participates in metal-ligand  $\pi$ -bonding. If a pseudooctahedral geometry is postulated, then metal d-electrons in the  $t_{2g}$  molecular orbitals overlap the  $\pi$ -bonding orbitals of the unsaturated pyridine ring. This represents an example of "back-bonding" where the flow of electron density is from the filled d-orbitals of the metal center to the ligand, the latter of which functions as a Lewis  $\pi$ -acid.<sup>11,12</sup> Of course, one requires that the  $\pi$ -bonding orbitals of the pyridine ring accept electron density from the metal center without deviating from planarity or resonance structures. Consequently, the carbon-nitrogen bond is strengthened when metal d-electron density flows into the aromatic  $\pi$ -bonding orbitals, and the "coordination" absorption band of the pyridine carbon-nitrogen stretch is observed 20 wavenumbers higher relative to the infrared absorption when coordination is absent. An analysis of the results from both spectroscopic techniques ( $^{13}\text{C}$  NMR and FTIR) suggests that coordination is operative in the amorphous phase between the zinc cation and the pyridine ring. The NMR discussion above pinpoints the zinc cation indirectly by focusing on the carboxylate carbon, two bonds removed from the coordination sites. In this section, the results from infrared spectroscopy pinpoint the ligand directly by probing vibrational motions that involve the pyridine-nitrogen site. The 1575–1600 wavenumber region of the infrared spectra in Figure 7 (a and b) contains overlapping vibrational absorptions from each component in the binary mixtures. This complication, which is prevalent throughout most of the FTIR spectrum, makes it difficult to detect unambiguously the uncomplexed (i.e., free) pyridine stretching vibration at 1596 wavenumbers in blends that contain excess polymer on a molar basis. In this respect, the site-specific molecular-level results from infrared spectroscopy are not correlated further, on a case-by-case basis, with the temperature-composition phase diagrams in Figures 1 and 3.

**Importance of d-Block Metallic Cations Categorized as Borderline Acids When Coordination with Pyridine Is Desired.** Magnesium Acetate and Poly(4-vinylpyridine). The ability of  $d^{10}$   $\text{Zn}^{2+}$  complexes to coordinate with pyridine ligands is emphasized from the concept of hard-and-soft acids and bases<sup>8</sup> in this section via comparison of zinc acetate-P4VP and magnesium acetate-P4VP solid solutions. Carbon-13 solid-state NMR spectra are presented in Figure 2 for blends that contain the borderline acid salt, zinc acetate. It was concluded that a coordination complex forms between the zinc cation and the accessible pyridine-nitrogen lone pair which is localized in the amorphous phase. The carboxylate carbon NMR signal in zinc acetate indirectly detects this blending-induced metal-ligand bond via line-shape broadening, and a progressive shift of the peak position to lower chemical shifts. In contrast, the spectroscopic data in Figure 8 reveal that the carboxylate  $^{13}\text{C}$  NMR signal of the hard-acid salt, magnesium acetate, in its undiluted state and in blends with P4VP, is not sensitive to the presence of the polymeric component. This provides one counterexample demonstrating that the borderline polymeric base, P4VP, favors coordination with borderline acids, such as  $\text{Zn}^{2+}$ , rather than hard acids such as  $\text{Mg}^{2+}$ . Infrared data are consistent with this counterexample because the aromatic carbon-nitrogen vibrational absorption of P4VP is found at 1596–1600  $\text{cm}^{-1}$  in blends with magnesium acetate,<sup>27</sup> indicative of a pyridine ligand that does not participate in  $\sigma$ -bonding

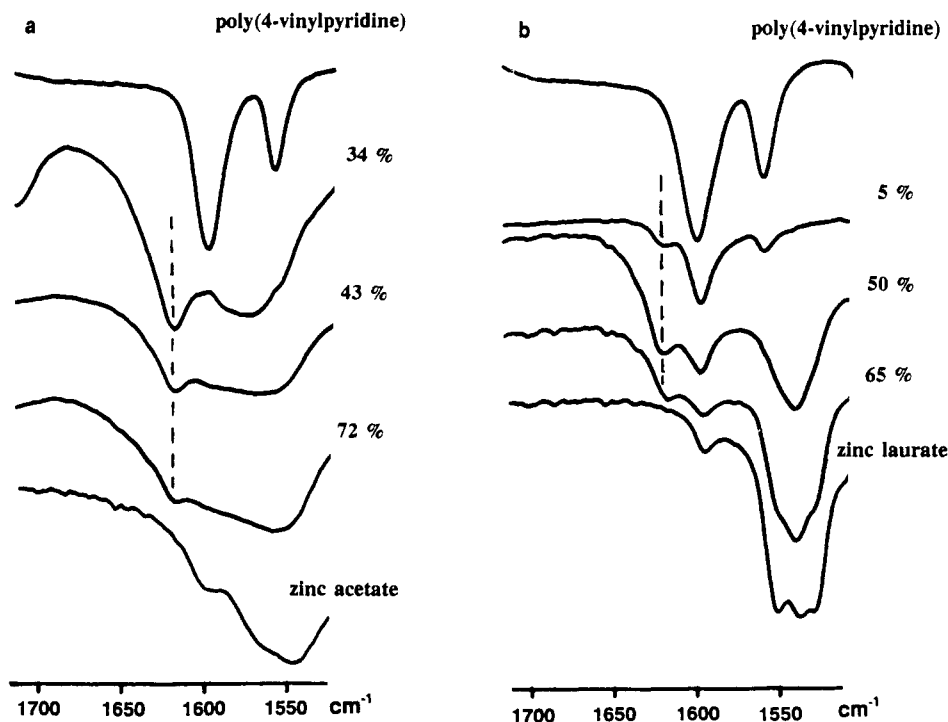


**Figure 7.** Fourier transform infrared spectra of binary mixtures containing poly(4-vinylpyridine) with (a) zinc acetate and (b) zinc laurate. The dashed line identifies the carbon-nitrogen stretching vibration unique to the pyridine ring when P4VP is coordinated to zinc. The mole percent of the zinc salt is indicated at the right of each infrared spectrum.

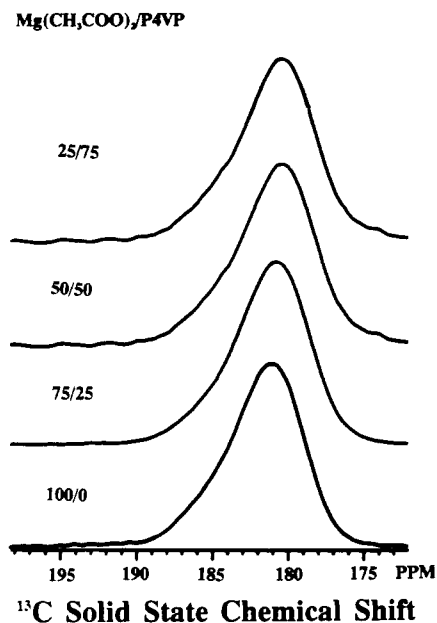


**Figure 8.** Carbon-13 solid-state NMR spectra in the carboxylate chemical shift region for binary mixtures of magnesium acetate and poly(4-vinylpyridine). The mole percent of magnesium acetate-P4VP is indicated at the left of each spectrum. The carboxylate signal of magnesium acetate is spectroscopically inert in all of the blends.

or  $\pi$ -bonding with the metal center. Macroscopic support for this claim is provided by the fact that concentration-independent melting is observed for magnesium acetate in blends with P4VP that contain 25–100 mol % of the hard-acid salt,<sup>26</sup> whereas no melting is detected in blends containing as much as 85 mol % zinc acetate (see Figure 1). Furthermore, the glass transition of poly(4-vinylpyridine) is weakly concentration dependent in blends with magnesium acetate,<sup>19,26</sup> exhibiting only a slight depression for the 50/50 blend relative to the undiluted polymer. As a second counterexample, blends of P4VP with the hard-

acid salt, calcium acetate, exhibit a glass transition temperature that is the same as the  $T_g$  of undiluted P4VP.<sup>34</sup> In contrast, synergistic glass transition response is observed in blends of P4VP with zinc acetate (see Figure 1).

The experimental results presented in Figures 1–8 stress the importance of chemical structure and the concept of hard-and-soft acids and bases<sup>8</sup> in the design of strongly interacting systems. Coordination complexes with poly(4-vinylpyridine) require that d-block metallic cations classified as borderline acids (e.g.,  $Zn^{2+}$  and  $Ni^{2+}$ <sup>34</sup>) be present in one of the components. The ligands should contain a lone pair that is not hindered sterically by other segments of the molecular chain. The results suggest that the molecular weight of the hydrocarbon tail in the zinc salts plays an important role in governing the one- vs two-phase behavior of the binary systems that were investigated. These concepts are employed in the following section to design polymer-ionomer blends that form coordination complexes and exhibit synergistic mechanical performance.

**Transition-Metal Complexation in Polymer-Ionomer Blends.** The overall goal of the research described in this section is to design high-molecular-weight blends, based on the concepts introduced above, that exhibit d-metal coordination and attractive macroscopic properties as a consequence of site-specific interactions. The polymeric ligand P4VP contains a nitrogenic lone pair that is structurally accessible. This follows directly from the model system investigations. The polymeric d-block metal-containing component (Surlyn 1706) mimics the small-molecule zinc salts by using the zinc cation to neutralize the methacrylic acid segments of an ethylene-methacrylic acid copolymer. This choice of components allows one to focus on the carboxylate carbon NMR signal in the *amorphous* domains of the ionic copolymer and obtain indirect spectroscopic detection of metal-ligand coordination. Direct detection of metal-ligand  $\pi$ -bonding is provided by infrared spectroscopy. Relative to the model systems that contain a low-molecular-weight component,

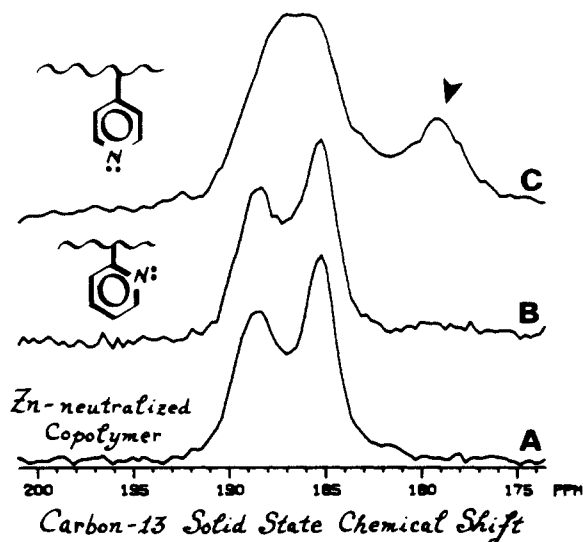


**Figure 9.** Carbon-13 solid-state NMR spectra in the carboxylate chemical shift region for Surlyn 1706 (A) in the undiluted state (the weight fraction of methacrylic acid in the ion-containing copolymer is 0.15 and  $\approx 60\%$  of the carboxylic acid groups are neutralized with zinc), (B) in a blend with 33 wt % poly(2-vinylpyridine), and (C) in a blend with 29 wt % poly(4-vinylpyridine). The arrow in spectrum C identifies the  $^{13}\text{C}$  NMR detectable carboxylate signal that arises when zinc coordinates to the pyridine ring via the nitrogen lone pair.

the choice of a polymeric ligand and a zinc-containing ionomer should enhance the potential for these high-molecular-weight blends to exhibit synergistic mechanical response.

The  $^{13}\text{C}$  NMR data in Figure 9 focus on the carboxylate signal of the partially neutralized ionic copolymer of ethylene and methacrylic acid in the 180–190 ppm chemical shift region of the spectrum. Partial neutralization of the methacrylic acid group produces an additional complexity in the carboxylate region that was not an issue for the blends containing low-molecular-weight zinc salts. This is illustrated in spectrum A where two carboxylate signals are well-resolved for the undiluted ionic copolymer. Previous investigations of the morphological and spectroscopic properties of copolymers and ionomers containing ethylene and methacrylic acid<sup>13,14</sup> have identified the unneutralized  $^{13}\text{COOH}$  resonance in spectrum A at 185 ppm and the neutralized  $^{13}\text{COOZn}$  signal at  $\approx 188$ –189 ppm. Hence, zinc neutralization of the carboxylate group produces an NMR-distinguishable effect on the carbon spectrum. On the basis of spectroscopic observations for model blends of zinc stearate and P2VP (see Figure 6), it is not surprising that the overall carboxylate resonance envelope of the ionomer is insensitive to the presence of P2VP as illustrated in spectrum B. When P2VP is replaced by P4VP and the nitrogenic lone pair becomes “structurally accessible”, the data in Figure 9C reveal that a new mixing-induced carboxylate signal appears in the vicinity of 179–180 ppm. Infrared data for polymer-ionomer blends of Surlyn 1706 and P4VP identify the coordination absorption band of P4VP’s aromatic carbon–nitrogen stretch at 1618 wavenumbers,<sup>27</sup> suggesting that metal–ligand  $\pi$ -bonding is operative. This is consistent with all of the results discussed above for the model P4VP–small molecule blends. Hence, spectroscopic observations indicate that coordination complexes between the ionic copolymer and P4VP are favorable to some extent, but some of the barriers that thwart complexation in P2VP–zinc stearate mixtures are prevalent also in these high-molecular-weight systems containing P4VP. In support of this latter claim, the carboxylate signal at 179–180 ppm

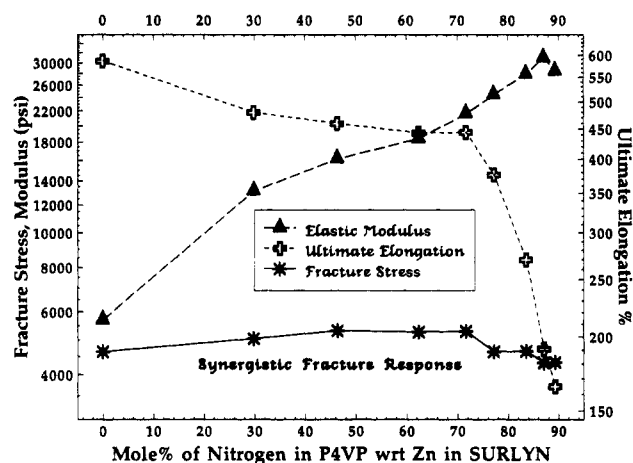


**Figure 10.** Mechanical properties of polymer-ionomer blends containing Surlyn 1706 and poly(4-vinylpyridine) as a function of P4VP concentration. A 15% increase in fracture response with respect to undiluted Surlyn 1706 is observed for blends which contain 46–72 mol % P4VP, where the concentration of Surlyn 1706 is based on the moles of zinc counterions. The ultimate elongation is greater than 440% for blends that exhibit synergistic fracture stress behavior.

that is indicative of metal–ligand coordination represents only a minor fraction of the overall line shape in spectrum C.

Mechanical properties in Surlyn 1706–P4VP solid-state blends are illustrated in Figure 10 as a function of P4VP concentration. It should be mentioned that data on the concentration axis are based on the moles of nitrogenic lone pairs and the moles of  $\text{Zn}^{2+}$ . Hence, if the weight fraction of Surlyn 1706 in the blend is designated by  $\omega$ , then  $\omega/1972$  represents the moles of  $\text{Zn}^{2+}$  and  $(1 - \omega)/105$  represents the moles of nitrogen. This formulation of the blend concentration variable allows one to identify a stoichiometric imbalance of one of the interacting groups. The properties of the undiluted ionic copolymer appear on the left side of Figure 10. A 5-fold increase in elastic modulus is observed relative to the modulus of Surlyn 1706 when one introduces the polymeric component that contains the pyridine ligand. This is understandable because P4VP exhibits a larger resistance to mechanical deformation. The properties of undiluted P4VP are difficult to measure because the polymer is quite brittle with low mechanical integrity when the molecular weight is in the range of 40 000. However, this “low-molecular-weight” P4VP (i) imparts stiffness to Surlyn 1706, (ii) enhances the fracture stress of the blends by  $\approx 15\%$ , and (iii) maintains an acceptable ultimate elongation of at least 440% when the concentration of nitrogen lone pairs is less than 72 mol %. Mechanical synergy is operative when one of the blend properties illustrated in Figure 10 exceeds the corresponding best pure-component property. In this respect, there is no synergistic response in ultimate elongation because Surlyn 1706 is more ductile (i.e.,  $\approx 600\%$  strain at failure) than all of the blends. The fracture strain of P4VP (MW = 40 000) is a few percent at best. The search for synergy in the elastic modulus is, most likely, overshadowed by the fact that P4VP is more resistant to mechanical deformation than Surlyn 1706. This suggests that the substantial improvement in blend moduli is strongly a consequence of the additive “rule of mixtures”. Verification of this claim is pending because of a lack of knowledge of the pure component mechanical properties of P4VP (MW = 40 000). Finally, the fracture stress of Surlyn 1706 is much higher than that of undiluted P4VP. The concentration dependence of the fracture response

suggests that this claim is justified even though pure-component properties were not measured for P4VP. The synergistic effect on fracture stress illustrated in Figure 10 is  $\approx 15\%$  relative to the fracture stress of undiluted Surlyn 1706 for blend concentrations between 46 and 72 mol % nitrogen. At higher concentrations of P4VP, the mechanical properties deteriorate markedly.

## Conclusions

The results presented in this contribution identify the coordination mechanism as an attractive route to produce solid-state blends that exhibit synergistic properties at the macroscopic level. Glass transition temperatures and mechanical fracture stresses were measured in excess of the best pure-component properties for poly(4-vinylpyridine) blends with zinc acetate and a zinc-neutralized ionomer, respectively. Molecular spectroscopy offers a useful diagnostic probe of these d-metal complexes. Infrared studies directly identify the fact that the pyridine nitrogen lone pair participates in metal-ligand  $\pi$ -bonding via a shift of the aromatic carbon-nitrogen stretching vibration to higher energy. Solid-state NMR focuses on the carboxylate carbon in the zinc salts and the ionic copolymer to provide indirect evidence for coordination. The chemical shift of the carboxylate carbon is very sensitive to microenvironmental factors that perturb its local electron density. Hence, it is possible to differentiate metal centers coordinated to acetate and pyridine ligands from metal centers coordinated to acetate and waters of hydration. The NMR results correlate quite well with macroscopic temperature-composition phase diagrams, suggesting that isotropic  $^{13}\text{C}$  chemical shifts are sensitive to phase coexistence when the "critical" component is present in both phases. In one particular case described herein, the carboxylate signal of zinc laurate identifies a disordered crystalline phase in low abundance that is not detected by differential scanning calorimetry, due to overlap between the glass and melting transitions. The concept of hard-and-soft acids and bases is useful to explain the fact that the hard acid  $\text{Mg}^{2+}$  preferentially coordinates to acetate anions and waters of hydration, which are classified as hard bases, instead of the borderline base poly(4-vinylpyridine). In agreement with this hypothesis, solid-state NMR reveals that the carboxylate  $^{13}\text{C}$  signal of magnesium acetate is spectroscopically inert, infrared spectroscopy does not detect the coordination absorption of P4VP's aromatic carbon-nitrogen stretch, and calorimetry identifies major differences between blends of (i) magnesium acetate with P4VP and (ii) zinc acetate with P4VP, the latter of which exhibits thermal synergy.

**Acknowledgment.** The research discussed herein was supported in full by the National Science Foundation (Grant MSM-8811107), the Colorado Advanced Materials Institute, Asahi Chemical Industries, and the Plastics Institute of America. We gratefully acknowledge the Colorado State University Regional NMR Center, funded by the National Science Foundation under Grant CHE-8746548, for providing instrumentation and professional assistance in obtaining the  $^{13}\text{C}$  solid-state NMR results. A.T.N.P. is grateful to CNPq (the National Research Council of Brazil) and the Federal University of Santa Catarina for a fellowship to conduct research while on

sabbatical at Colorado State University. E.U. acknowledges Asahi Chemical Industries in Okayama, Japan, for research support as a visiting scientist in the United States.

## References and Notes

- (1) Wissbrum, K. F.; Hannon, M. J. *J. Polym. Sci., Polym. Phys. Ed.* 1975, 13, 223.
- (2) Agnew, N. H. *J. Polym. Sci., Polym. Chem. Ed.* 1976, 14, 2819.
- (3) Register, R. A.; Weiss, R. A.; Li, C.; Cooper, S. L. *J. Polym. Sci., Part B: Polym. Phys.* 1989, 27, 1911.
- (4) Peiffer, D. G.; Duvdevani, I.; Agarwal, P. K.; Lundberg, R. D. *J. Polym. Sci., Polym. Lett. Ed.* 1986, 24, 581.
- (5) Agarwal, P. K.; Duvdevani, I.; Peiffer, D. G.; Lundberg, R. D. *J. Polym. Sci., Polym. Phys. Ed.* 1987, 25, 839.
- (6) Pires, A. T. N.; Cheng, C.; Belfiore, L. A. *ACS Proc. Div. Polym. Mater. Sci. Eng.* 1989, 61, 466.
- (7) Valero Capilla, A.; Alcala Aranda, R. *Cryst. Struct. Commun.* 1979, 8, 795.
- (8) Pearson, R. G. In *Survey of Progress in Chemistry—Volume 6*; Scott, A., Ed.; Academic Press: New York, 1969; Chapter 1.
- (9) March, J. *Advanced Organic Chemistry*, 3rd ed.; Wiley: New York, 1985.
- (10) Gutmann, V. *Coordination Chemistry in Nonaqueous Solutions*; Springer-Verlag: Berlin, 1968.
- (11) Shriver, D. F.; Atkins, P. W.; Langford, C. H. *Inorganic Chemistry*; W. H. Freeman: New York, 1990, Chapter 7.
- (12) Figgis, B. *An Introduction to Ligand Fields*; Wiley: New York, 1966.
- (13) Belfiore, L. A.; Shah, R. J.; Cheng, C. *Contemporary Topics in Polymer Science, Volume 6, Multiphase Macromolecular Systems*; Culbertson, B. M., Ed.; Plenum Press: New York, 1989; p 619.
- (14) Belfiore, L. A.; Lutz, T. J.; Cheng, C. *Solid State NMR Detection of Molecular-Level Mixing Phenomena in Strongly Interacting Polymer Blends and Phase-Separated Copolymers. Solid State NMR of Polymers*; Mathias, L., Ed.; Plenum Press: New York, 1991; Chapter 8.
- (15) Wind, R. A.; Anthonio, F. E.; Duijvestijn, M. J.; Smidt, J.; Trommel, J.; DeVette, G. M. C. *J. Magn. Reson.* 1983, 52, 424.
- (16) Stejskal, E. O.; Schaefer, J. J. *Magn. Reson.* 1975, 18, 560.
- (17) Earl, W. L.; VanderHart, D. L. *J. Magn. Reson.* 1982, 48, 35.
- (18) Moore, W. J. *Physical Chemistry*, 4th Ed.; Prentice-Hall: Englewood Cliffs, NJ, 1972; p 751.
- (19) Ueda, E., unpublished results.
- (20) de Meftahi, M. V.; Frechet, J. M. J. *Polymer* 1988, 29, 477.
- (21) Kwei, T. K. *J. Polym. Sci., Polym. Lett. Ed.* 1984, 22, 306.
- (22) Lin, P. Y.; Clash, C.; Pearce, E. M.; Kwei, T. K.; Aponte, M. A. *J. Polym. Sci., Polym. Phys. Ed.* 1988, 26, 603.
- (23) Yang, T. P.; Pearce, E. M.; Kwei, T. K.; Yang, N. L. *Macromolecules* 1989, 22, 1813.
- (24) Lin, A. A.; Kwei, T. K.; Reiser, A. *Macromolecules* 1989, 22, 4112.
- (25) Wang, L. F.; Pearce, E. M.; Kwei, T. K. *J. Polym. Sci., Polym. Phys. Ed.* 1991, 29, 619.
- (26) Pires, A. T. N., unpublished results.
- (27) Wang, Y. M.S. Thesis, Colorado State University, 1991.
- (28) Patwardhan, A. A.; Belfiore, L. A. *Polym. Eng. Sci.* 1988, 28 (14), 916.
- (29) Cheng, C. M.S. Thesis, Colorado State University, 1989.
- (30) Qin, C.; Pires, A. T. N.; Belfiore, L. A. *Polym. Commun.* 1990, 31, 177.
- (31) Belfiore, L. A.; Qin, C.; Pires, A. T. N.; Ueda, E. *Polym. Prepr. (Am. Chem. Soc., Div. Polym. Chem.)* 1990, 31 (1), 170.
- (32) Qin, C.; Belfiore, L. A. *Polym. Prepr. (Am. Chem. Soc., Div. Polym. Chem.)* 1990, 31 (1), 263.
- (33) Van Niekerk, J. N.; Schoening, F. R. L.; Talbot, J. H. *Acta Crystallogr.* 1953, 6, 720.
- (34) Belfiore, L. A.; Graham, H.; Ueda, E. *Ligand Field Stabilization in Nickel Complexes That Exhibit Extraordinary Glass Transition Temperature Enhancement*. Submitted for publication in *Macromolecules*.

**Registry No.** P2VP, 25014-15-7; P4VP, 25232-41-1;  $\text{Zn}(\text{O}_2\text{CCH}_3)_2(\text{H}_2\text{O})_2$ , 557-34-6;  $\text{Zn}(\text{O}_2\text{CC}_{11}\text{H}_{23})_2$ , 2452-01-9;  $\text{Zn}(\text{O}_2\text{CC}_{18}\text{H}_{37})_2$ , 557-05-1;  $\text{Mg}(\text{O}_2\text{CCH}_3)_2(\text{H}_2\text{O})_4$ , 142-72-3; Surlyn 1706, 28516-43-0.